

07,01

## ***In situ* investigation of the mechanism of propagation of Portevin–Le Chatelier deformation bands**

© A.A. Shibkov, A.E. Zolotov, M.F. Gasanov, A.A. Denisov, R.Yu. Koltsov

Tambov State University,  
Tambov, Russia

E-mail: shibkovaleks@mail.ru

Received March 21, 2023

Revised March 21, 2023

Accepted March 28, 2023

Based on the analysis of high-speed video data of propagating deformation bands in an aluminum-magnesium alloy, it was found that the movable deformation band contains an excess of dislocations of one mechanical sign, and the main mechanism for the propagation of the localized plastic deformation front along the sample axis is a relay transmission of sliding in the antiparallel direction to relax the bending moment created by the primary deformation band. It is shown that the „instantaneous“ rate of plastic deformation during  $\sim 1$  ms in the growing band reaches a value of  $\sim 10^3$  s $^{-1}$ , comparable to the rate of deformation during shock tests.

**Keywords:** intermittent deformation, vocalization, dislocations, mechanical charge, aluminum-magnesium alloy.

DOI: 10.21883/PSS.2023.05.56051.39

### **1. Introduction**

Many structural metals and alloys exhibit intermittent deformation expressed in repeated stress or strain jumps during testing with given strain rate ( $\dot{\varepsilon}_0 = \text{const}$ ) or stress rate ( $\dot{\sigma}_0 = \text{const}$ ), respectively — the Portevin–Le Chatelier (PLC) effect [1]. Microscopic stress or strain jumps are followed by localization of plastic deformation in bands. Their origin and propagation mechanism have been a matter of argument for a long time [2–5]. To study the spontaneous deformation band formation mechanism, information is required on the earliest deformation band evolution stages, including initiation, features of transverse growth, dynamic interaction with other bands and surface, etc., which required considerable increase in response time and spatial resolution of methods of *in situ* study of PLC deformation bands. Over the previous three decades, the time resolution of the methods has increased by more than three orders of magnitude — from 25 to 50000 frames per second, fps, while the spatial resolution has increased by almost one order of magnitude (from  $\sim 100$  to  $\sim 10$   $\mu\text{m}/\text{pixel}$ ) [6–10]. This allowed to detect nucleation bands growing across the sample in uniaxial strain conditions, to detect a band self-acceleration stage, measure maximum band tip rates, etc. Recently, studies have appeared that addressed the first millisecond of deformation band evolution as an individual subject of research using video recording at a rate of at least 5000 fps [7–11]. This study investigates the features of nucleation band dynamics in flat samples with growth of width-to-thickness ratio, in particular in very thin samples, where deformation bands several hundreds microns in width may exhibit internal structure associated with the mechanism of interaction between the adjacent material layers in the band. The purpose of this study is to investigate the mechanism of PLC deformation band propagation on

the basis of analysis of high-speed video records of band dynamics on aluminum-magnesium alloy — AlMg6 — demonstrating intermittent deformation and band formation at room temperature.

### **2. Procedure**

Commercial aluminum-magnesium alloy — AlMg6 — is the test material: Al — 6.15% Mg — 0.65% Mn — 0.25% Si — 0.21% Fe — 0.1% Cu — 0.12% Zn (wt.%). Flat samples of various thickness  $w_0$  from 100 to 500  $\mu\text{m}$  in the form of double-sided blades with working section  $S_0 = 6 \times 3$  mm were machined from a cold-rolled strip in rolling direction. Before testing, the samples were annealed at 450°C during 1 h and quenched in air. Average grain size after heat treatment was about 10  $\mu\text{m}$ . Investigations of alloy microstructure and a set of high-speed deformation and loading methods as well as tension scheme are described in [12–14].

Behavior and morphology of propagating deformation bands were investigated *in situ* by video recording of the deformation sample surface in oblique light at a rate of 5000 fps using FASTCAM Mini UX50/100 (Photron) high-speed video camera. Video record processing involved subtraction of successive in time video frames using computer software. Such image processing method allows to identify outlines of moving objects (deformation bands and cracks) at a rate higher than a threshold value. The loading procedure and deformation band recording was described in detail in [14].

### **3. Results and discussion**

*In situ* study of deformation band dynamics and morphology in flat samples of various thickness shows that

deformation band width  $w_b$  at active development stage is compared with sample thickness  $w_b \approx 1.5w_0$ . Therefore, with decreasing sample thickness the band width decreases

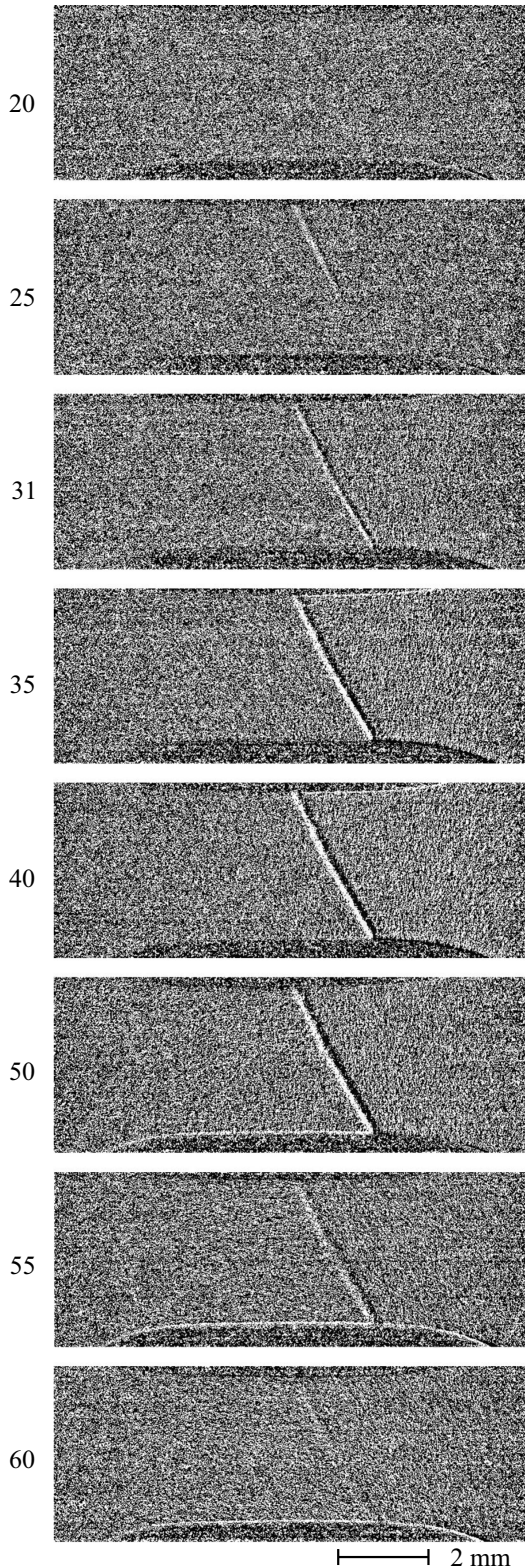


**Figure 1.** Fragment of video record of a bent deformation band in a flat AlMg6 alloy sample with  $6 \times 3 \times 0.12$  mm working part. Video recording rate 5000 fps. Numbers — frame numbers.

proportionally and at thicknesses lower than  $200 \mu\text{m}$  internal band structure starts manifesting itself (recorded shadow band behavior test method) due to its splitting, path distortion, etc. The study of phenomena associated with distortion of bands is essential, because bending of a sample with a moving deformation band is directly associated with excess of dislocations of the same mechanical sign in the band structure which can be assessed from high-speed video recording data. The main results of the „in situ“ study of early evolution stages for individual deformation bands in  $120 \mu\text{m}$  samples.

Figure 1 shows a fragment of video record of deformation band initiation and growth which changes the propagation angle across the sample. After initiation on a side surface of the sample, the band first propagates at  $\varphi_1 = 60^\circ$  to the tension axis (frame 25) close to the direction of maximum tangential stresses (for isotropic material undergoing plastic deformation, this angle is  $54^\circ 44'$  [15]). Then, in the sample center, the angle between the band and tension axis decreases up to  $\varphi_2 = 55^\circ$  (frames 35–50) in such a way that band angle  $\Delta\varphi = \varphi_2 - \varphi_1$  is about  $5^\circ$  (Figure 2). Slip direction turning is correlated with excessive dislocations of the same mechanical sign by a known relation [16]:

$$\bar{\rho}_{\text{exc}} = \frac{1}{bR} = \frac{\Delta\varphi}{bl_b \cos \varphi}, \quad (1)$$

where  $\bar{\rho}_{\text{exc}} = \bar{\rho}_+ - \bar{\rho}_-$  is the difference of average dislocation densities of different mechanical signs,  $b$  is the Burgers vector,  $R$  is the deformation band curvature radius,  $l_b = \Delta\varphi R$  is the band length,  $\varphi = (\varphi_1 + \varphi_2)/2$  is the angle between the neutral line and deformation band. Expression (1) assumes that dislocations are evenly distributed over the crystal. Correlation between  $\bar{\rho}_{\text{exc}}$  and excessive dislocations of the same mechanical sign in macrolocalized band  $\rho_b^{\text{exc}}$  is defined by the obvious relation (see [17]):

$$\rho_b^{\text{exc}} = \bar{\rho}_{\text{exc}} V_0 / V_b, \quad (2)$$

where  $V_0$  is the volume of the sample working part,  $V_b$  is the deformation band volume. Since PLC bands pass through entire flat samples as shown by video recording using two mirrors [18], then  $V_b = S_b w_0$ , where  $S_b$  is the band area and  $V_0 / V_b = S_0 / S_b = S_0 / l_b w_b$ , and finally we obtain

$$\rho_b^{\text{exc}} = \frac{\Delta\varphi S_0}{bl_b^2 w_b \cos \varphi}. \quad (3)$$

Substituting typical experimental values:  $\Delta\varphi = 5^\circ = 8.72 \cdot 10^{-2}$  rad,  $S_0 = 6 \times 3 = 18 \text{ mm}^2$ ,  $w_b \approx 200 \mu\text{m}$ ,  $l_b \approx 4 \text{ mm}$ ,  $b = 0.286 \text{ nm}$ ,  $\varphi \approx 60^\circ$ ,  $\cos \varphi \approx \sqrt{3}/2$ , excessive density of mobile dislocations of the same mechanical sign is estimated as  $\rho_b^{\text{exc}} \approx 3 \cdot 10^8 \text{ cm}^{-2}$ .

Deformation band initiation and development is followed by unloading jump of machine–sample mechanical system. When the band stops, its immobile dislocations with density  $\rho_+ + \rho_-$  become dislocation movement locks and

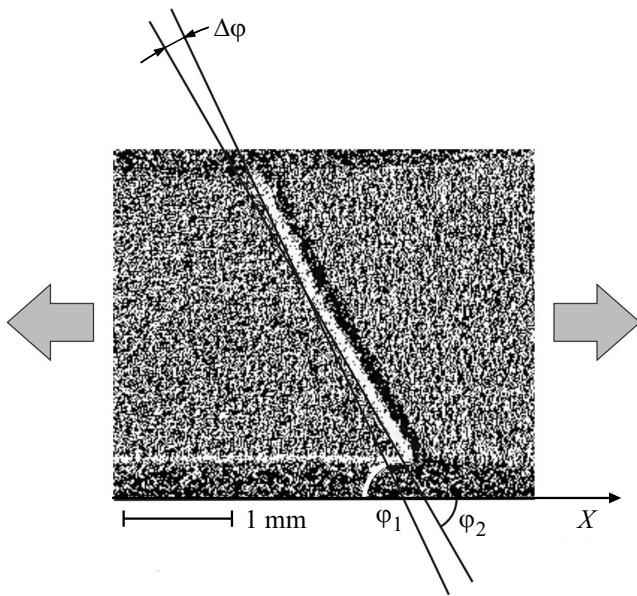


**Figure 2.** Change of deformation band growth direction (frame 50 on Figure 1).  $\varphi_1 = 55^\circ$  and  $\varphi_2 = 60^\circ$  are start and final inclination angle of the deformation band to the tension axis  $X$ .

contribute to the Taylor hardening of the material by an order of magnitude of (stress drop) amplitude

$$\Delta\sigma = \alpha mbG \cdot \sqrt{\rho_+ + \rho_-}, \quad (4)$$

where  $m$  is the Taylor factor (for FCC polycrystals  $m = 3.08$  [19]),  $\alpha$  is the interdislocation interaction constant defining the shear strength which depends on the dislocation structure; for Al–Mg system alloys with magnesium content 3–6%  $\alpha = 0.36–0.45$  [20],  $G = 28$  GPa is the shear modulus. From equation (4), estimate of the density of stopped dislocations in the band is derived  $\rho_b = \rho_+ + \rho_- = (\Delta\sigma/\alpha mbG)^2$ . Substituting typical values for AlMg6  $\alpha = 0.45$ ,  $\Delta\sigma \approx 15–20$  MPa, estimate  $\rho_b \approx (2–3.2) \cdot 10^8 \text{ cm}^{-2}$  is derived, which is better than by an order of magnitude coincides with the excessive dislocation density of the same sign, i.e.  $\rho_b \approx \rho_{exc}$ ; hence  $\rho_+ \gg \rho_-$ .

Therefore, a deformation band propagating across the sample in the maximum tangential stress direction contains mobile dislocations primarily of the same mechanical sign with density  $\rho_b \approx 3 \cdot 10^8 \text{ cm}^{-2}$ , which allows to estimate the plastic deformation rate in the band  $\dot{\epsilon}_b$  at the incomplete growth stage which is characterized by tip rate  $v_t$  and side growth rate  $v_s$  of the band [9]. Assuming that dislocation rate in the band  $v_d$  is not lower than the band tip rate, i.e.  $v_d \approx v_t$ , the lower estimate is as follows  $\dot{\epsilon}_b$ :

$$\dot{\epsilon}_b \approx b\rho_b v_t. \quad (5)$$

In thin samples ( $w_0 \approx 100–200 \mu\text{m}$ ) at stresses  $\sigma \approx 200–250$  MPa, the average tip rate is  $v_t \approx (1–2)$  m/s, which gives an estimate of plastic deformation rate in the band  $\dot{\epsilon}_b \approx (0.86–1.7) \cdot 10^3 \text{ s}^{-1}$  during the first millisecond

of its growth and, thus, the estimate of peak with respect to the strain in the band  $\epsilon_b \approx 1$ . Such high local (in space and time) strain and strain rates are specific to impact tests [21].

It is important that incomplete (embryo) band, due to the excessive dislocations of the same sign, represents a mechanical charge — source of long-range elastic stress

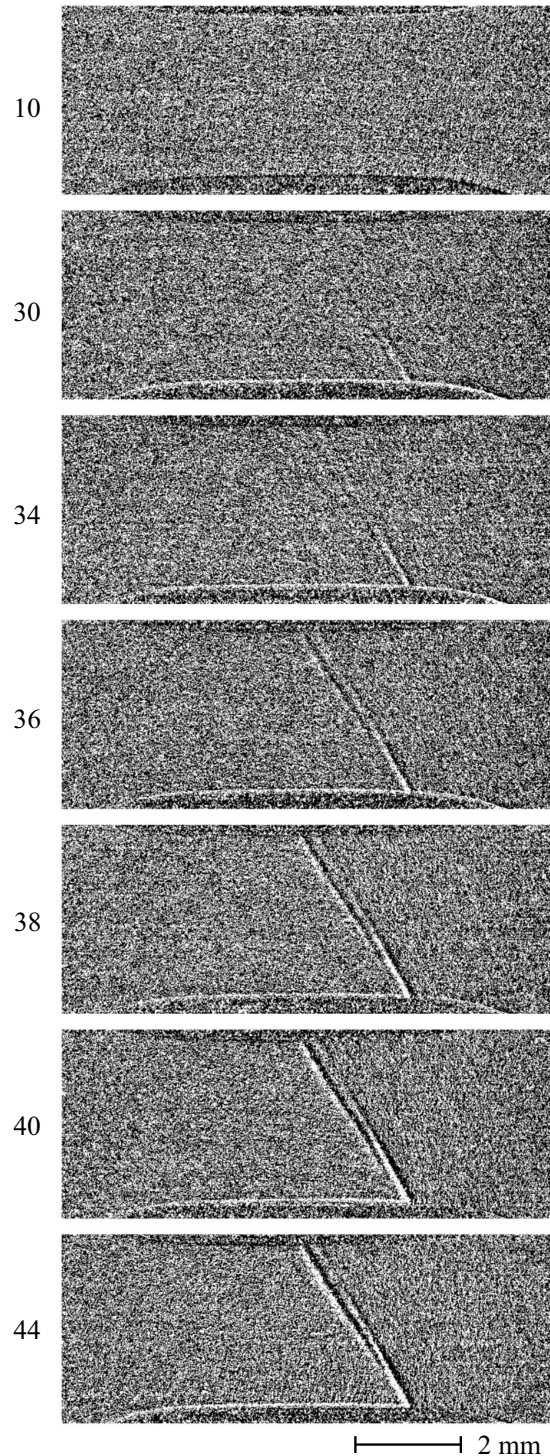


**Figure 3.** Fragment of video record demonstrating band „reradiation“ by the surface when the secondary band propagates antiparallel to the primary band. Video recording rate — 5000 fps.

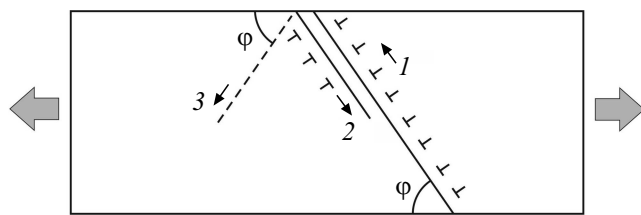


**Figure 4.** Diagram of shift forwarding associated with bending moment relaxation: 1 — primary band; 2 — secondary band propagating antiparallel to the primary band; 3 — conjugate direction of maximum tangential stresses.

fields in the material. This mechanical charge generates the bending moment in the sample which may be compensated due to initiation and propagation of the deformation band with excessive dislocations of the opposite mechanical sign. Figure 3 shows a fragment of video record demonstrating such mechanism.

The primary band is initiated on the side surface (frame 30, image bottom) and propagates at a rate of  $\sim 1$  m/s. Band width by the time, when the opposite side surface is achieved, is about  $200 \mu\text{m}$ . Approaching the opposite side surface, the deformation band with its long-range elastic field initiates the dislocation source which generates a deformation band in the antiparallel direction. The secondary band contains excessive dislocations of the opposite sign (because it moves in the opposite direction at the same applied stress) and compensates the bending moment generated by the primary band. The diagram of this process is shown in Figure 4, where the bands containing excessive dislocations of one sign (mechanical charges) growing in the polycrystalline material are shown schematically as flat pile-ups of similarly charged dislocations.

As the secondary band develops, the distance from the primary bands decreases from  $\sim 400$  to  $\sim 250 \mu\text{m}$  at about 4 mm (Figure 3, frames 36–44), which may be explained by the attraction of the opposite signs of the secondary and primary bands. However, annihilation of these dislocations is unlikely, because the standard distance between them is dozens of times longer than the average grain size and, therefore, probability of interaction of mobile dislocations with „non-transparent“ grain boundaries (with unfavorable Schmid factor) is very high.

Thus, using *in situ* experiments, it was found that the main macroscopic mechanism of deformation band expansion is slip motion forwarding in antiparallel direction due to generation of dislocations by a surface source in the secondary band containing excessive dislocations of the opposite sign for relaxation of the bending moment generated by the primary band.

Among the space coupling mechanisms discussed in literature, a mechanism of double cross slip (DCS) of screw dislocations [22] and mechanisms associated with slip activation by excessive shear stress at the deformation band front [3] shall be highlighted. Due to relatively low

transverse slip  $h_s \approx 1\text{--}10$  nm, the DCS mechanism can explain the thin structure and expansion rate of lines and slip bands (micro- and mesolevel) in metals [17], but to understand the mechanism of slip transfer at a distance of dozens and hundreds of microns, mechanisms of slip activation by long-range stress fields are preferable.

Elastic accommodation at the interface of a plastic deformation layer and strain-free layer in the material is the most common cause of excess stresses at the deformation band. In [18] it is shown that various gradient ductility theories give the estimate of the same magnitude regarding the width of a layer of highly nonuniform plastic deformation — band boundary „width“ — where excess stresses are concentrated,  $l \approx 10\text{--}20 \mu\text{m}$ . Excess stress in the gradient layer with width  $l$  facilitate propagation of the secondary deformation band. Alternative scenario of bending moment relaxation from the primary band, when the secondary nucleation band of the opposite mechanical sign is formed in the conjugate direction (direction 3 in Figure 4), is apparently less probable compared with the nucleation band growing antiparallel to the primary band (direction 2 in Figure 4), because in the latter case: a) the most efficient shielding is provided for long-range stress fields generated by the primary band; b) excess shear stresses at the primary band boundary create favorable conditions for propagation of the secondary band.

## 4. Conclusion

High-speed investigations of the Portevin–Le Chatelier early deformation band formation stage were carried out on  $\sim 100 \mu\text{m}$  thick aluminum-magnesium alloy flat samples. By the detected curvature of the nucleation band growth direction, density of excessive dislocations of the same mechanical sign  $\sim 3 \cdot 10^8 \text{ cm}^{-2}$  and „instant“ within  $\sim 1$  ms peak plastic deformation rate in the band, that achieves  $\sim 10^3 \text{ s}^{-1}$ , comparable with the impact test strain rate, were estimated. „Line“ mechanism of band expansion was detected, where achievement of the surface by the primary band initiates the secondary band generation process in antiparallel direction to compensate for the bending moment generated by the primary band. The line mechanism, thus, ensures forwarding of the shear plastic deformation to the adjacent layers of the material and is responsible for expansion of the completed deformation band.

## Funding

This study was supported by the Russian Science Foundation (project No. 22-22-00692) using the equipment of the Center of Equipment Sharing of Derzhavin TGU.

## Conflict of interest

The authors declare that they have no conflict of interest.

## References

- [1] J.F. Bell. Eksperimental'nye osnovy mekhaniki deformiruemyykh tverdykh tel. P. 2 Nauka, M. (1984). 432 p. [J.F. Bell. Mechanics of Solids. Springer (1972). V. 2.]
- [2] P. Hahner, A. Ziegenbein, E. Rizzi, H. Neuhauser. Phys. Rev. B **65**, 13, 134109 (2002).
- [3] P. Hahner. Scripta Metallurgica. Mater. **29**, 9, 1171 (1993).
- [4] G. Ananthakrishna. Dislocations in Solids / Eds F.R.N. Nabarro, J.P. Hirth (2007). V. 13. P. 81.
- [5] A.J. Yilmaz. Sci. Technol. Adv. Mater. **12**, 6, 063001 (2011).
- [6] K. Chihab, Y. Estrin, L.P. Kubin, J. Vergnol. Scripta Metallurgica **21**, 2, 203 (1987).
- [7] W. Tong, H. Tao, N. Zhang, L.G. Hector Jr. Scripta Materialia **53**, 1, 87 (2005).
- [8] M.M. Krishtal, A.K. Khrustalev, A.V. Volkov, S.A. Borodin. Dokl. Phys. **54**, 5, 225 (2009).
- [9] A.A. Shibkov, M.A. Zheltov, M.F. Gasanov, A.E. Zolotov, A.A. Denisov, M.A. Lebyodkin. Mater. Sci. Eng. A **772**, 138777 (2020).
- [10] A.A. Shibkov, M.A. Lebyodkin, T.A. Lebedkina, M.F. Gasanov, A.E. Zolotov, A.A. Denisov. Phys. Rev. E **102**, 4, 043003 (2020).
- [11] A.A. Shibkov, A.E. Zolotov, M.F. Gasanov, A.A. Denisov, R.Yu. Kol'tsov, S.S. Kochegarov. FTT **64**, 11, 1603 (2022). (in Russian).
- [12] A.A. Shibkov, A.A. Mazilkin, S.G. Protasova, D.V. Mikhlik, A.E. Zolotov, M.A. Zheltov, A.V. Shuklinov, Deformatsiya i razrushenie materialov, **6**, 5 (24) (in Russian).
- [13] A.A. Shibkov, A.E. Zolotov, D.V. Mikhlik, M.A. Zheltov, A.V. Shuklinov, V.A. Averkov, A.A. Denisov. Deformatsiya i razrushenie materialov, **6**, 8 (23) (in Russian).
- [14] A.A. Shibkov, M.F. Gasanov, M.A. Zheltov, A.E. Zolotov, V.I. Ivolgin. Int. J. Plast. **86**, 37 (2016).
- [15] R. Hill. The Mathematical Theory of Plasticity. Clarendon Press, Oxford (1951).
- [16] J. Friedel. Dislocations. Elsevier (1964).
- [17] H. Neuhauser. Dislocation in Solids / Ed. F.R.N. Nabarro. North Holland Company **6**, 319 (1983).
- [18] A.A. Shibkov, A.E. Zolotov, M.A. Zheltov. Phys. Solid State **52**, 11, 2376 (2010).
- [19] U.F. Kocks. Am. Soc. Mech. Eng. J. Eng. Mater. Tech **98**, 1, 76 (1976).
- [20] N.A. Koneva, E.V. Kozlov. V sb.: Perspektiv. materialy / Pod red. D.L. Merson. TGU, MISIS, M., (2006). p. 267. (in Russian).
- [21] N.S. Selyutina, Yu.V. Petrov. Phys. Solid State **60**, 2, 244 (2018).
- [22] V. Jeanclaude, C. Fressengeas. Scripta Metallurgica **29**, 9, 1177 (1993).

*Translated by E.Ilyinskaya*